BMB
Reports

BMB Rep. 2024; 57(3): 161-166
www.bmbreports.org

Exploring the DNA methylome of Korean patients with colorectal cancer consolidates the clinical implications of cancer-associated methylation markers

Sejoon Lee[1,#], Kil-yong Lee[2,#], Ji-Hwan Park[3,4,#], Duck-Woo Kim[5], Heung-Kwon Oh[5], Seong-Taek Oh[2], Jongbum Jeon[3], Dongyoon Lee[3], Soobok Joe[3], Hoang Bao Khanh Chu[6], Jisun Kang[6], Jin-Young Lee[6], Sheehyun Cho[6], Hyeran Shim[6], Si-Cho Kim[6], Hong Seok Lee[6], Young-Joon Kim[6], Jin Ok Yang[3,], Jaeim Lee[2,*] & Sung-Bum Kang[5,*]*

[1]Precision Medicine Center, Seoul National University Bundang Hospital, Seongnam 13620, [2]Department of Surgery, Uijeongbu St. Mary's Hospital, College of Medicine, The Catholic University of Korea, Uijeongbu 11765, [3]Korea Bioinformation Center (KOBIC), Korea Research Institute of Bioscience and Biotechnology, Daejeon 34141, [4]Department of Bioscience, University of Science and Technology (UST), Daejeon 34113, [5]Department of Surgery, Seoul National University Bundang Hospital, Seoul National University College of Medicine, Seongnam 13620, [6]Department of Biochemistry, College of Life Science and Biotechnology, Yonsei University, Seoul 03722, Korea

Aberrant DNA methylation plays a critical role in the development and progression of colorectal cancer (CRC), which has high incidence and mortality rates in Korea. Various CRC-associated methylation markers for cancer diagnosis and prognosis have been developed; however, they have not been validated for Korean patients owing to the lack of comprehensive clinical and methylome data. Here, we obtained reliable methylation profiles for 228 tumor, 103 adjacent normal, and two unmatched normal colon tissues from Korean patients with CRC using an Illumina Infinium EPIC array; the data were corrected for biological and experiment biases. A comparative methylome analysis confirmed the previous findings that hypermethylated positions in the tumor were highly enriched in CpG island and promoter, 5′ untranslated, and first exon regions. However, hypomethylated positions were enriched in the open-sea regions considerably distant from CpG islands. After applying a CpG island methylator phenotype (CIMP) to the methylome data of tumor samples to stratify the CRC patients, we consolidated the previously established clinicopathological findings that the tumors with high CIMP signatures were significantly enriched in the right colon. The results showed a higher prevalence of microsatellite instability status and *MLH1* methylation in tumors with high CMP signatures than in those with low or non-CIMP signatures. Therefore, our methylome analysis and dataset provide insights into applying CRC-associated methylation markers for Korean patients regarding cancer diagnosis and prognosis. [BMB Reports 2024; 57(3): 161-166]

*Corresponding authors. Sung-Bum Kang, Tel: +82-31-787-7087; Fax: +82-31-787-4077; E-mail: kangsb@snubh.org; Jaeim Lee, Tel: +82-31-820-5020; Fax: +82-31-847-2041; E-mail: lji96@catholic.ac.kr; Jin Ok Yang, Tel: +82-42-879-8550; Fax: +82-42-879-8519; E-mail: joy@kribb.re.kr
#These authors contributed equally to this work.

https://doi.org/10.5483/BMBRep.2023-0103

**Received 19 June 2023, Revised 26 July 2023,
Accepted 13 November 2023, Published online 12 March 2024**

Keywords: Colorectal cancer, CpG island methylator phenotype, DNA methylation, Microsatellite instability, MutL homolog 1 (*MLH1*)

INTRODUCTION

DNA methylation plays a crucial role in colorectal cancer (CRC) tumorigenesis as it regulates the methylation of regulatory elements of tumor suppressor genes or oncogenes and affects gene expression (1-3). For example, high microsatellite instability (MSI-H) resulting from *MLH1* promoter hypermethylation has been linked to CRC prognosis and immune checkpoint inhibitors (4, 5). Furthermore, systematic methylation profiling of patients with CRC has revealed that a CpG island methylator phenotype (CIMP) can be reflected in the widely accepted molecular classification of CRC (6-10). This classifies the cancer type into four consensus molecular subtypes, characterized by overall hypermethylation, intermediate methylation, and low methylation throughout the genome (8).

The Cancer Genome Atlas (TCGA) provides multi-omics data, including methylome data on CRC. However, methylation markers have common or race-specific characteristics (11), making it challenging to understand the CRC characteristics in the Korean population from TCGA alone, which primarily contains data from Caucasian patients. Nevertheless, several studies on Korean patients with CRC have generated genome data from the tumor and adjacent normal tissues of the patients (12, 13). Thus, an unmet need for methylome data exists to confirm the effectiveness of methylation profiling-based subtyping in Korean patients with CRC.

ISSN: 1976-670X (electronic edition)

To this end, we aimed to establish a comprehensive methylome dataset from Korean patients with CRC and systematically investigated the characteristics of methylation profiles in these patients. The associated data provide detailed groups with distinct clinicopathological and molecular characteristics, which will help determine the optimal therapy and develop more effective CRC prevention and treatment strategies.

RESULTS

Correction of sex- and batch-related biases provides highly harmonized data

We collected data from 228 Korean patients with CRC and obtained clinical information, such as sex, age, tumor location, and MSI status (Supplementary Table 1 and Supplementary Fig. 1). For methylation profiles of Korean patients with CRC, we evaluated the quality of the EPIC array data by inspecting the overall distribution of beta values and control strip plots, including the bisulfite conversion efficiency, extension quality, and specificity (Supplementary Fig. 2). We acquired 609,046 probe methylation beta values from 228 tumors and 105 normal samples for downstream analysis. Through statistical data exploration, including normalization and filtering, we obtained high-quality harmonized data and effectively eliminated technical noise and sex-based biases (Supplementary Figs. 3 and 4).

Differentially methylated positions in tumor tissues show distinct distribution in genic and CpG island-associated regions

In the principal component analysis plot (Fig. 1A), a clear separation between tumor and normal samples was observed while analyzing the 609,046 processed methylation datasets. Notably, the grand mean methylation level of 609,046 probes across all normal samples was slightly higher than that across tumor samples (0.5824 and 0.5570 for normal and tumor samples, respectively; Fig. 1B). Subsequently, we identified 38,607 differentially methylated positions (DMPs) between the tumor and normal samples (Supplementary Table 2) and found approximately four times more hypomethylated positions (30,783 probes) than hypermethylated positions (7,824 probes) in the tumor samples (Fig. 1C, D). For each DMP group, we calculated the odds ratio of enrichment for hyper- and hypomethylated positions for various genomic annotations, including gene promoter-like regions, body regions, and islands or shores. In promoter-like regions (TSS1500, TSS200, 5′-untranslated region [UTR], and first exon), the odds ratios between the number of

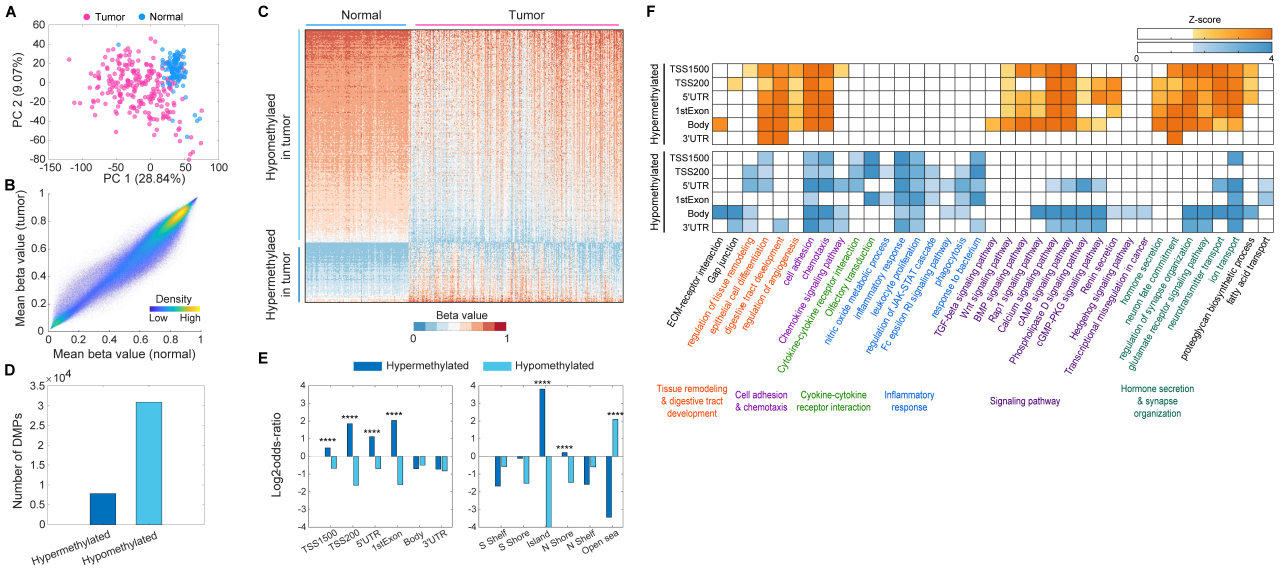

Fig. 1. Identification of differentially methylated positions between tumor and normal tissues. (A) Principal component (PC) analysis of 228 tumors (red) and 105 normal tissue samples (blue) using the preprocessed 609,046 methylation probes. The plot shows the PC1 (x-axis) and PC2 (y-axis) with their explained variances. (B) Scatter plot showing mean beta values of the 609,046 methylation probes across normal (x-axis) and tumor samples (y-axis). (C) Heat map describing hypo- and hypermethylated positions in the tumor tissue samples, compared with normal tissue samples. For better visualization, we randomly selected 5% of the differentially methylated positions (DMPs) and performed a hierarchical clustering with the application of Euclidean distance and the average linkage method. The color bar denotes the gradient of beta values as a measurement of methylation level. (D) Number of total DMPs between the tumor and normal tissue samples. (E) Bar graph of $\log_2$-odds-ratios representing the enrichment significance of the DMPs for each of the genic (left) and CpG-island-associated regions (right). ****P $<$ 0.0001 by the empirical statistical test as described in Supplementary Methods and Materials. (F) Heat map showing the functional enrichment patterns of GOBPs and KEGG pathways by hyper- and hypomethylated positions at genomic regions (TSS1500, TSS200, 5′-UTR, first exon, body, and 3′-UTR). Color bar, gradient of Z-score for the enrichment P-value computed by using DAVID software.

observed and expected hypermethylated positions were 1.3972, 3.5963, 4.1059, and 2.1671, respectively ($P < 0.0001$; Supplementary Table 3, top and Fig. 1E, left). Hypermethylated positions were highly enriched in CpG island and N shore regions (Supplementary Table 4, bottom and Fig. 1E, right), with an odds ratio of 13.9850 for CpG island regions ($P < 0.0001$). In contrast, hypomethylated positions in tumor samples were primarily found in open-sea (odds ratio: 4.2877, $P < 0.0001$) regions (Supplementary Table 4, bottom and Fig. 1E), which are considerably distant from the CpG island regions.

To understand cellular processes and signaling pathways epigenetically regulated by the DMPs, we performed a functional enrichment analysis of Gene Ontology Biological Processes (GOBP) and Kyoto Encyclopedia of Genes and Genomes (KEGG) pathways for the hyper- and hypomethylated positions located at TSS1500, TSS200, 5′-UTR, first exon, body, and 3′-UTR regions (Fig. 1F). We found that (i) angiogenesis, signaling pathways (TGF-beta, Wnt, and BMP signaling pathways), hormone secretion, and neuron fate commitment were significantly ($P < 0.05$) enriched by only the hypermethylated positions; (ii) cytokine-cytokine receptor interaction (olfactory transduction), inflammatory response (nitric oxide metabolic process, leukocyte proliferation, JAK-STAT cascade, Fc epsilon RI signaling pathway, phagocytosis, and response to bacterium), Hedgehog signaling pathway, transcriptional misregulation in cancer, and fatty acid transport were enriched by only the hypomethylated positions; (iii) ECM-receptor interaction, gap junction, tissue remodeling and digestive tract development (epithelial cell differentiation), cell adhesion and chemotaxis (chemokine signaling pathway), signaling pathways (Rap1, calcium, cAMP, phospholipase D, and cGMP-PKG signaling pathways and renin secretion), synapse organization (glutamate receptor signaling pathway and neurotransmitter and ion transport), and proteoglycan biosynthetic process were enriched by hyper- and hypomethylated positions. Moreover, the comparison with the enrichment P-values for negative control positions (see details in Supplementary Materials and Methods) implied that the enriched GOBPs and KEGG pathways were predominantly regulated by the DMPs (Fig. 1F and Supplementary Fig. 5). Notably, among the GOBPs and KEGG pathways enriched by hyper- and hypomethylated

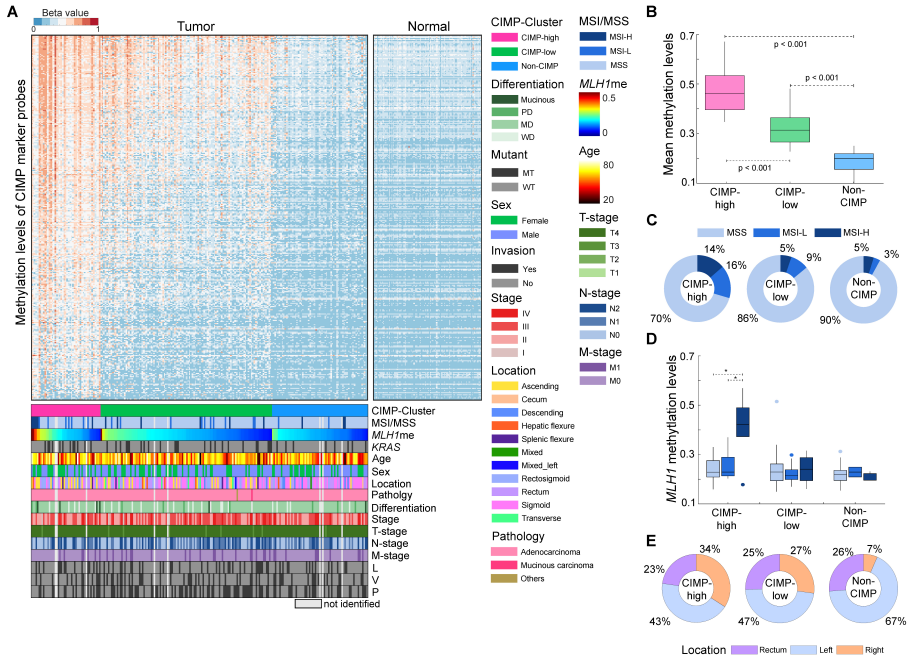

Fig. 2. Clustering of 228 colon tumor samples according to the CpG island methylator phenotype (CIMP). (A) Clustering of 228 colon tumor and 105 normal tissue samples based on the methylation levels of the CIMP marker probes. For the visualization of the heatmap, the samples (column) in each of the CIMP groups were sorted according to *MLH1* methylation level. For each of the 16 clinicopathological characteristics (CIMP cluster, microsatellite instability [MSI] status, *MLH1* methylation, *KRAS* mutation, age, sex, location, pathology, differentiation, stage, and T-, N-, and M-stages, and lymphatic [L], venous [V], and perineural [P] invasions), the samples without relevant information ("not identified") appear bright gray in the heatmap. (B) Boxplot showing mean beta values of CIMP marker probes for the patient groups classified according to their CIMP status. (C) Proportion of patients with MSI-low and -high, and microsatellite stability (MSS) statuses for each of the CIMP groups. (D) Boxplot showing the distribution of *MLH1* beta values for the patient groups classified according to their CIMP and MSI statuses. (E) Distribution of tissue location for each of the CIMP groups. The boxes in (B) and (D) display the lower, median, and upper quartiles; the whiskers represent the minimum and maximum values. *$P < 0.05$ by one-way ANOVA with a post hoc test (Sidak correction).

positions, ECM-receptor interaction, TGF-beta and Hedgehog signaling pathways, and transcriptional misregulation in cancer were enriched by only the DMPs located at body regions. This finding supports that methylation-associated epigenetic regulation of the body region plays a distinct role in CRC development compared to the promoter-like region, as described in previous studies (2, 14). Collectively, these results suggest that our DNA methylome data may provide valuable insights into CRC biology.

Integrative analysis of CIMP reveals DNA methylation-associated clinicopathological implications for Korean patients with CRC

To interpret the clinicopathological characteristics of Korean patients with CRC based on their methylation profiles, we assessed the prevalence of CIMP. The 228 tumor samples were clustered into three groups with respect to the methylation levels in the 1,470 CIMP probe set derived from 258 previously identified CIMP gene markers (15) (see details in Supplementary Materials and Methods) (Fig. 2A). We confirmed the significant (ANOVA with a post hoc test, $P < 0.001$) changes in the mean methylation levels of the CIMP marker probes between the three groups (Fig. 2B). We then investigated whether there were clinicopathological differences across the three groups (Supplementary Table 1). There were no significant differences in the age (ANOVA, $P = 0.448$), sex (Chi-square test, $P = 0.517$), tumor AJCC stage (Fisher's exact test, $P = 0.641$), T (Fisher's exact test, $P = 0.109$), N (Chi-square test, $P = 0.514$), or M (Chi-square test, $P = 0.956$) stages or the differentiation status (poorly, moderately, and well-differentiated states and mucinous status; Fisher's exact test, $P = 0.174$) distributions between the CIMP groups. Additionally, we examined the association between survival and CIMP status by conducting a relapse-free survival analysis for the patients stratified by CIMP status. We ascertained that the patients in the CIMP-H exhibited a significantly (Log-rank test, hazard ratio = 2.215 and P-value < 0.05) poorer outcome than their counterparts (*i.e.*, CIMP-L and non-CIMP; Supplementary Fig. 6).

Among the 228 patients with CRC, 220 were tested for genetic mutations (Supplementary Table 1), 44 (20.0%) of them had *KRAS* mutations. However, there were no significant differences in the distribution of *KRAS* (Chi-square test, $P = 0.175$) mutations among the CIMP groups. Microsatellite instability (MSI) status was available for 220 patients; the frequency of MSI-H tumors in the CIMP-H group (13.6%) was significantly (Fisher's exact test, $P = 0.041$) higher than that in the CIMP-L (5.3%) and non-CIMP (4.8%) groups (Fig. 2C and Supplementary Table 1). To address the shared features of the patients with MSI-H status in the CIMP-H group, we investigated the methylation levels of *MLH1*—a DNA mismatch repair gene in which the hypermethylation of the promoter is associated with MSI in CRC (4). The *MLH1* methylation levels were higher in the CIMP-H group (mean methylation: 0.26) than in the CIMP-L (mean methylation: 0.23) and non-CIMP (mean methylation: 0.22) groups (*T*-test [CIMP-H vs. non-CIMP-H], $P < 0.05$, see *MLH1* methylation levels in Supplementary Fig. 7A). The CIMP-H group exhibited a significant association between *MLH1* methylation and MSI-H status (Fig. 2D). The mean *MLH1* methylation level of patients with CIMP-H and MSI-H status (0.41) was significantly (ANOVA with a post hoc test, $P < 0.001$) higher than that of patients with CIMP-H and MSS (0.25) or MSI-L status (0.24); however, the mean methylation levels of all CIMP markers did not significantly differ with the MSI status of CIMP-H patients (Supplementary Fig. 8).

Tumor location data were available for 212 patients; the distribution was as follows: 113 (53.3%) on the left side (descending, rectosigmoid, sigmoid, and splenic flexure) of the colon, 55 (25.9%) in the rectum, and 44 (20.8%) on the right side (ascending, cecum, and hepatic flexure) of the colon (Fig. 2E and Supplementary Table 1). In the CIMP-H group, 15 tumor samples (34%) were found on the right side of the colon and 29 (66%) on the left side. In contrast, only 25 (22%) and 4 (7%) right colon tumors were observed in the CIMP-L and non-CIMP groups, respectively. These results showed significant enrichment (Chi-square test, $P = 0.006$) of tumor samples on the right colon in the CIMP-H group, suggesting that the CIMP status was correlated with the anatomical location within the large intestine. Collectively, DNA methylation profiling of CIMP markers and *MLH1* was highly associated with MSI status and tumor location as well as relapse-free survival, rather than other clinicopathological features in CRC patients.

Previously known CIMP markers were associated with the clinicopathological implications of Korean CRC methylome data. However, the markers did not fully represent our DMPs and *vice versa*. For example, when we compared the methylation levels of the probes annotated with the promoter-like regions of 11 previously identified CIMP marker genes (7), the methylation levels of the ten genes were significantly (*T*-test, $P < 0.05$) higher in the CIMP-H group than in the CIMP-L and non-CIMP groups. However, the methylation levels of *SOCS1* were not significantly changed (Supplementary Fig. 7A). Thus, we sought to identify a set of novel CIMP marker candidates representing the DMPs. To this end, we first selected 680 of the 7,824 hypermethylated positions in the tumor tissues (see details in Supplementary Materials and Methods). These positions could stratify patients into three discrete categories, which concurred with our pre-established CIMP classifications (Supplementary Fig. 7B, C). After the refining process for the 680 positions, we prioritized 16 positions as novel CIMP marker candidates, showing significant (P-value < 0.0001) changes in mean methylation levels between the patients with CIMP-H, CIMP-L, and non-CIMP status (Supplementary Fig. 9 and Supplementary Table 5; see details in Supplementary Materials and Methods).

DISCUSSION

We investigated alterations in the DNA methylation levels in

228 patients with CRC and their potential associations with clinicopathological features. Our analysis of a large methylation dataset comprising 609,046 probes revealed a clear distinction between tumor and normal samples, indicating significant differences in methylation levels between the groups. We also identified 38,607 DMPs between the tumor and normal samples, with more hypomethylated positions in the tumor samples. Hypermethylated positions were primarily found in the gene promoter-like and CpG island regions, and hypomethylated positions were exclusively detected in the open-sea regions.

Our study embarked on a comprehensive exploration of DMPs to elucidate their biological relevance in CRC. While we initially highlighted the significance of overrepresented genes in GOBP and KEGG pathways, we expanded our analysis by investigating specific genes pivotal to CRC progression (Supplementary Table 6). A salient finding from our study is the hypermethylation of genes such as *SFRP1*, *SFRP2*, *SOX17*, and *WIF1*, shedding light on their antagonistic roles in the WNT signaling pathway and their consequent significance in CRC (16). Of particular note is the *SMAD* family, which plays a central role in the signal transduction of the TGF-β superfamily (17, 18). This family encompasses TGF-βs, bone morphogenetic proteins, and activins. The observed hypermethylation of *SMAD1* and *SMAD2* in CRC underscores a potential dysregulation of the TGF-β signaling pathway (19, 20), warranting further investigation. Our findings concerning *ADAMTSs* resonate with existing literature, emphasizing their nuanced roles across various cancers (21-23). The diverse expression of *ADAMTSs*, particularly the involvement of *ADAMTS1* in colon cancer cachexia, emphasizes their relevance in CRC (24). Their multifunctional roles, from tumor-protective effects to interactions with the extracellular matrix, are pivotal. Observations of genetic aberrations, whether mutations or epigenetic silencing in ADAMTS genes, align with broader oncological research (23). *CDH13* emerged as another critical gene in our study. Given its established role in cell recognition and adhesion, its methylation pattern in CRC could herald early oncogenic processes (25). Our findings on *TMEFF2* (26), *ADCY1* (27), and *ADCY4* (28) hypermethylation complement and extend the existing cancer research, linking them to cell adhesion and cAMP signaling pathways. By placing these findings with other omics-based studies, we aim to cultivate a holistic understanding of the molecular intricacies underpinning CRC progression.

We also examined the prevalence of CIMP and stratified the patients into three groups (CIMP-H, CIMP-L, and non-CIMP) based on their mean methylation levels for a set of previously known CIMP marker probes. We observed a significant enrichment of patients with MSI-H within the CIMP-H group, and the *MLH1* methylation levels were higher in the CIMP-H group than in the other two groups. This significant association between *MLH1* methylation level and MSI-H status in the CIMP-H group supports a combinatorial assessment of CIMP status and *MLH1* methylation level as a promising measurement predicting MSI status of CRC, as suggested by previous studies (29).

The CIMP status was correlated with not only patient relapse-free survival but also the anatomical location of the large intestine, with an enrichment of right colon tumors in the CIMP-H group. Our results are similar to those of previous studies (6, 30). In particular, right-sided colon cancer has a poorer oncological prognosis than left-sided colon cancer (31). Considering the distinct cancer prognosis as per the tumor location, a methylation profiling of tumor samples may be necessary to infer the location and establish a proper treatment plan. Collectively, these results support the previous findings on CRC-associated methylation characteristics, which may facilitate a personalized approach to cancer diagnosis and prognosis.

Our findings provide novel insights into the epigenetic alterations associated with CRC and their potential clinical implications. For example, we suggested potential CRC diagnostic markers commonly used for other ethnic groups as well as the novel CIMP marker candidates, which may be associated with several clinicopathological characteristics. The enrichment of hypermethylated positions in the gene promoter-like and CpG island regions suggests that these regions play a crucial role in the development of CRC. The observed associations among CIMP status, MSI status, and *MLH1* methylation level suggest that these biomarkers have prognostic value in patients with CRC. We also highlight the importance of considering the anatomical location of tumors when evaluating epigenetic alterations in colon cancer, as we observed a significant association between the CIMP status and tumor location in the large intestine. In comparison with TCGA CRC dataset, although our cohort contained a disproportionate amount of samples from later stages than early stages (Supplementary Table 7, $P < 0.001$), this profiling could provide an opportunity to investigate markers of poor prognosis. Further studies are required to validate our findings and elucidate the mechanisms underlying these epigenetic alterations in CRC.

MATERIALS AND METHODS

Ethical statement

This study was approved by Seoul National University Bundang Hospital Institutional Review Board (approval number: B-1709-423-306), Uijeongbu St. Mary's Hospital Institutional Review Board (approval number: XC17TNDI0068), and Yonsei University Institutional review board (approval number: 7001988-201910-BR-727-02).

Data availability

The raw IDAT files and processed methylation profiles are available in Korea BioData Station (K-BDS, https://kbds.re.kr/) with the accession ID PRJKA2086326 (32). The raw CRC methylome of TCGA was downloaded from The Genomic Data Commons portal (https://portal.gdc.cancer.gov/repository).

ACKNOWLEDGEMENTS

This research was supported by the Bio & Medical Technology Development Program (grant number: NRF-2017M3A9A7050614, NRF-2017M3A9A7050610 and NRF-2023M3A9A7009442) and the Korea BioData Station Program.

CONFLICTS OF INTEREST

The authors have no conflicting interests.

REFERENCES

1. Das PM and Singal R (2004) DNA methylation and cancer. J Clin Oncol 22, 4632-4642
2. Lakshminarasimhan R and Liang G (2016) The role of DNA methylation in cancer. Adv Exp Med Biol 945, 151-172
3. Nishiyama A and Nakanishi M (2021) Navigating the DNA methylation landscape of cancer. Trends Genet 37, 1012-1027
4. Herman JG, Umar A, Polyak K et al (1998) Incidence and functional consequences of hMLH1 promoter hypermethylation in colorectal carcinoma. Proc Natl Acad Sci U S A 95, 6870-6875
5. Zhao P, Li L, Jiang X and Li Q (2019) Mismatch repair deficiency/microsatellite instability-high as a predictor for anti-PD-1/PD-L1 immunotherapy efficacy. J Hematol Oncol 12, 54
6. Zlobec I, Bihl M, Foerster A, Rufle A and Lugli A (2011) Comprehensive analysis of CpG island methylator phenotype (CIMP)-high, -low, and -negative colorectal cancers based on protein marker expression and molecular features. J Pathol 225, 336-343
7. Nazemalhosseini Mojarad E, Kuppen PJ, Aghdaei HA and Zali MR (2013) The CpG island methylator phenotype (CIMP) in colorectal cancer. Gastroenterol Hepatol Bed Bench 6, 120-128
8. Guinney J, Dienstmann R, Wang X et al (2015) The consensus molecular subtypes of colorectal cancer. Nat Med 21, 1350-1356
9. Singh MP, Rai S, Pandey A, Singh NK and Srivastava S (2021) Molecular subtypes of colorectal cancer: an emerging therapeutic opportunity for personalized medicine. Genes Dis 8, 133-145
10. Joe S, Kim J, Lee JY et al (2023) Epigenetic insights into colorectal cancer: comprehensive genome-wide DNA methylation profiling of 294 patients in Korea. BMB Rep 56, 563-568
11. Galanter JM, Gignoux CR, Oh SS et al (2017) Differential methylation between ethnic sub-groups reflects the effect of genetic ancestry and environmental exposures. eLife 6, e20532
12. Jeon SA, Ha YJ, Kim JH et al (2022) Genomic and transcriptomic analysis of Korean colorectal cancer patients. Genes Genomics 44, 967-979
13. Lee SH, Lee B, Shim JH et al (2019) Landscape of actionable genetic alterations profiled from 1,071 tumor samples in Korean cancer patients. Cancer Res Treat 51, 211-222
14. Yang X, Han H, De Carvalho DD, Lay FD, Jones PA and Liang G (2014) Gene body methylation can alter gene expression and is a therapeutic target in cancer. Cancer Cell 26, 577-590
15. McInnes T, Zou D, Rao DS et al (2017) Genome-wide methylation analysis identifies a core set of hypermethylated genes in CIMP-H colorectal cancer. BMC Cancer 17, 228
16. Silva AL, Dawson SN, Arends MJ et al (2014) Boosting Wnt activity during colorectal cancer progression through selective hypermethylation of Wnt signaling antagonists. BMC Cancer 14, 891
17. Guo X and Wang XF (2009) Signaling cross-talk between TGF-beta/BMP and other pathways. Cell Res 19, 71-88
18. Huang F and Chen YG (2012) Regulation of TGF-beta receptor activity. Cell Biosci 2, 9
19. Ding N, Luo H, Zhang T, Peng T, Yao Y and He Y (2023) Correlation between SMADs and colorectal cancer expression, prognosis, and immune infiltrates. Int J Anal Chem 2023, 8414040
20. Hata A and Chen YG (2016) TGF-beta signaling from receptors to Smads. Cold Spring Harb Perspect Biol 8, a022061
21. Wagstaff L, Kelwick R, Decock J and Edwards DR (2011) The roles of ADAMTS metalloproteinases in tumorigenesis and metastasis. Front Biosci (Landmark Ed) 16, 1861-1872
22. Choi JE, Kim DS, Kim EJ et al (2008) Aberrant methylation of ADAMTS1 in non-small cell lung cancer. Cancer Genet Cytogenet 187, 80-84
23. Lind GE, Kleivi K, Meling GI et al (2006) ADAMTS1, CRABP1, and NR3C1 identified as epigenetically deregulated genes in colorectal tumorigenesis. Cell Oncol 28, 259-272
24. Cal S and López-Otín C (2015) ADAMTS proteases and cancer. Matrix Biol 44-46, 77-85
25. Hibi K, Kodera Y, Ito K, Akiyama S and Nakao A (2004) Methylation pattern of CDH13 gene in digestive tract cancers. Br J Cancer 91, 1139-1142
26. Yan H, He J, Guan Q et al (2017) Identifying CpG sites with different differential methylation frequencies in colorectal cancer tissues based on individualized differential methylation analysis. Oncotarget 8, 47356-47364
27. Zhang Y, Yang J, Wang X and Li X (2021) GNG7 and ADCY1 as diagnostic and prognostic biomarkers for pancreatic adenocarcinoma through bioinformatic-based analyses. Sci Rep 11, 20441
28. Fan Y, Mu J, Huang M et al (2019) Epigenetic identification of ADCY4 as a biomarker for breast cancer: an integrated analysis of adenylate cyclases. Epigenomics 11, 1561-1579
29. Jass JR (2007) Classification of colorectal cancer based on correlation of clinical, morphological and molecular features. Histopathology 50, 113-130
30. Sugai T, Habano W, Jiao YF et al (2006) Analysis of molecular alterations in left- and right-sided colorectal carcinomas reveals distinct pathways of carcinogenesis: proposal for new molecular profile of colorectal carcinomas. J Mol Diagn 8, 193-201
31. Petrelli F, Tomasello G, Borgonovo K et al (2017) Prognostic survival associated with left-sided vs right-sided colon cancer: a systematic review and meta-analysis. JAMA Oncol 3, 211-219
32. Lee B, Hwang S, Kim PG et al (2023) Introduction of the Korea BioData Station (K-BDS) for sharing biological data. Genomics Inform 21, e12